

# IMPLEMENTATION OF SATELLITE FORMATION FLIGHT ALGORITHMS USING SPHERES ABOARD THE INTERNATIONAL SPACE STATION

Christophe P. Mandy<sup>1</sup>

*Massachusetts Institute of Technology, Cambridge, MA 02139, USA*

Hiraku Sakamoto<sup>2,5</sup>

*Nihon University, Funabashi, Chiba 274-8501 Japan*

*and*

Alvar Saenz-Otero<sup>3</sup>, David W. Miller<sup>4</sup>

*Massachusetts Institute of Technology, Cambridge, MA 02139, USA*

**The MIT's Space Systems Laboratory developed the Synchronized Position Hold Engage and Reorient Experimental Satellites (SPHERES) as a risk-tolerant spaceborne facility to develop and mature control, estimation, and autonomy algorithms for distributed satellite systems for applications such as satellite formation flight. Tests performed study interferometric mission-type formation flight maneuvers in deep space. These tests consist of having the satellites trace a coordinated trajectory under tight control that would allow simulated apertures to constructively interfere observed light and measure the resulting increase in angular resolution. This paper focuses on formation initialization (establishment of a formation using limited field of view relative sensors), formation coordination (synchronization of the different satellite's motion) and fuel-balancing among the different satellites.**

## I. Introduction

Space interferometers are seen as one of the key ways to extend our knowledge of the universe. In the development of more powerful telescopes, astronomers recognize some great advantages interferometers provide over classical reflecting telescopes, particularly their potential to achieve greater resolution with smaller separated mirrors. Several missions such as NASA's TPF-I or ESA's DARWIN plan to send interferometers composed of distributed apertures in space. The general scheme is to have several separated satellites flying in a tightly controlled formation reflecting light to a combiner spacecraft where the light collected is interfered (see Fig. 1). The resolution of such a telescope is proportional to its baseline which is simply the distance between the different apertures in the formation. As a result, very large resolutions are possible which could only otherwise be achieved by sending very large monolithic telescopes to space or by assembling telescope mirrors in space from smaller sections launched separately to account for the limited size of current launch vehicle payload fairings. Typical interferometer formations require the different apertures to describe circular or spiral trajectories in a plane perpendicular to the line of sight to the object observed [1], but results presented in this paper can be applied to any formation flight mission.

This paper focuses on three key aspects of formation flight missions: formation acquisition, fuel balancing and synchronization. Section II describes MIT's ground- and space-based formation flight testbed: SPHERES. Section III presents formation acquisition techniques and experimental results: the way to allow the different component spacecraft of a formation to recognize each other before moving into formation, right after having been placed in

---

<sup>1</sup> Research Assistant, Space Systems Laboratory, newtoni@mit.edu

<sup>2</sup> Postdoctoral Fellow, Department of Aerospace Engineering, College of Science and Technology

<sup>3</sup> Research Scientist, Space Systems Laboratory

<sup>4</sup> Director, Space Systems Laboratory

<sup>5</sup> H. Sakamoto was supported by the Japan Society for the Promotion of Science, Postdoctoral Fellowships for Research Abroad 2005.

orbit by a launch vehicle. Section IV discusses fuel balancing techniques that allow spacecraft to generate trajectories that optimize mission duration by regulating fuel consumption then outlines maneuver synchronization techniques in a formation that require little computation and interspacecraft communication. Section V concludes and presents future work possibilities.

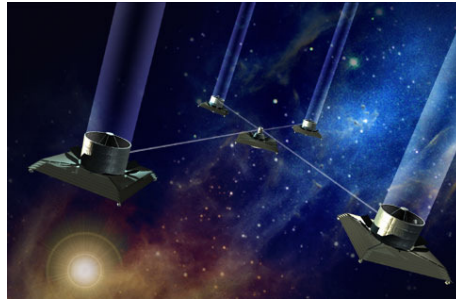


Figure 1: Artist's Conception of NASA's TPF-I mission [1]

## II. The SPHERES testbed



Figure 2: SPHERES satellite

The SPHERES (Synchronized Position, Hold, Engage, Reorient Experimental Satellites) testbed consists of six identical nano-satellites designed to demonstrate and mature control, estimation and formation flight algorithms in a fault-tolerant environment [3]. Three SPHERES are currently in the Space Station and operated by astronauts, while the other three are kept at MIT for ground testing. The satellites are actuated by 12 cold-gas thrusters operating with CO<sub>2</sub>, compute algorithms on-line and are capable of intersatellite and satellite-to-laptop communication. The SPHERES contain 3 gyroscopes and 3 accelerometers, and can also determine their position using an infrared and ultrasound-

based metrology system. The satellites are equipped with ultrasound and infrared sensors all around their structure. Each satellite also disposes of infrared emitters and a single ultrasound beacon centered on one of their faces. Five ultrasound beacons are attached to the space station's frame. To measure position, a satellite first emits an infrared ping in all directions. When this is received by one of the beacons attached to the ISS or by another satellite, the beacons will reply an ultrasound signal. Each beacon is assigned a specific time delay before replying so as to allow individual identification of the source of ultrasound signals. From the time-delay between the infrared ping and the ultrasound reply and by determining which ultrasound sensors received the reply, satellites can determine range and bearing information to the different beacons. In this manner, two metrology "modes" are possible: relative metrology, where satellites determine the position of other spacecraft relative to them (in their "body frame"), based on the ultrasound reply received from other SPHERES, and global metrology, where the satellites determine their position relative to the ISS (in the "global frame"), emulating a GPS device.



Figure 3: Astronaut Sunita Williams operating SPHERES on ISS (March 2007)

Algorithms are first tested on MIT's 3 degrees of freedom flat table facility where they are evolved to a space-testable level. Software is then sent to the Space Station to allow astronauts to test the designed experiments in the Space Station's microgravity environment. Astronauts operate three SPHERES within a volume defined by the five metrology beacons, communicating with the satellites via a laptop. In this manner, algorithms can be tested in an iterative manner, basing innovations on methods that have been tested. High-risk experiments can be attempted at low cost as any malfunction can be immediately tented to by the astronauts. Control and estimation algorithms and autonomy architectures can be run to the limits of their operability and tested for robustness without loss of precious hardware, while providing unique data on operation in a full 6 degrees of freedom environment. This procedure maximizes science time and limits overhead time by facilitating the modification of algorithms and their implementation on hardware. The process can then be iterated to allow for algorithms and formation-flight methods to be matured, optimized and improved for space applications.

### III. Formation Initialization

#### A. Overview

For real formation-flying satellites, when no high-accuracy terrestrial navigation aids like GPS are available, the satellites will be required to capture the formation using only relative position measurements, though the global attitude knowledge may be obtained by using a star tracker. This “formation initialization” problem has been theoretically discussed by some researchers and some simulations were carried out [4-6]. However, hardware implementation in either 2D or 3D has rarely been reported yet. The present study demonstrates formation-initialization maneuvers using SPHERES facility in the 3D ISS environment.

The formation-initialization procedure discussed herein consists of the following four stages.

(1) The multiple satellites are deployed without a prior knowledge of the other satellites’ positions (“Lost-in-space”), emulating a release from a launch vehicle or a case of contingency.

(2) The satellites capture the other satellites within their relative sensor range, which typically has a limited field-of-view (FOV).

(3) The satellites null their range rates.

(4) The satellites position themselves within an array.

In MIT’s March 2007 ISS test session, the first two stages, (1) and (2), were considered as the first step in tests for the development of formation-initialization techniques employing only two SPHERES. Figure 3 shows a picture taken during the ISS test session.

As described in Section II, each SPHERES satellite has an onboard ultrasound (U/S) transmitter, which emulates a sensor of an actual system with a limited FOV. Also 24 U/S receivers (4 on each of 6 faces) equip the satellites, enabling the satellite to receive the U/S signal from any direction. The satellites use an omnidirectional communication channel for the satellite-to-satellite communication. With these setups, two kinds of search strategies were tested in the session. First, satellites used relative sensing data as well as the satellite’s attitude information with respect to the global coordinate frame fixed to the ISS, in order to capture the other satellite in the middle of its U/S signal range (called “global search” hereafter). Second, satellites used only relative sensing data and no global attitude information (“relative search”). In both strategies, the search maneuvers were tested without initial relative velocity first, and later a moderate initial velocity was added to one of the two satellites to increase the complexity of the problem.

Two different strategies, global search and relative search, were developed and tested in the session for the following reason. In the global search, the positions of each satellite are measured relatively with respect to each satellite’s body coordinate, and at the same time the attitude of the satellites is measured with respect to the global coordinate system. The attitude control with respect to the global coordinate will be necessary when there are sun-angle constraints to protect the onboard sensitive devices, or tracking requirements for the sun, the earth or other objects. Thus, in this study, the search maneuver for the global search was designed to keep the angle between the body  $z$ -axis and the inertial  $Z$ -axis less than 60 deg as displayed in Figure 7(a). In addition, once the both satellites capture the partner, both satellites use the global attitude information so that the body  $z$ -axis in the final attitude makes the minimum angle from the inertial  $Z$  axis. Namely, the present global search strategy is to demonstrate the use of the combination of relative position measurements and the global attitude measurement for the formation initialization. On the other hand, in the relative search, no global attitude knowledge is used for the formation initialization. In this case, since each satellite has only one U/S transmitter onboard, the relative estimation using the single U/S signal does not provide information in the rotational direction about the body  $x$ -axis. As a result, in the final configuration, their rotational orientations about the  $x$ -axis are not necessarily aligned while the two satellites do point the U/S transmitter ( $-x$ ) face toward the other satellite. This present relative search strategy demonstrates the formation initialization with a minimal number of signal transmitters and sensors. The following two subsections describe the detailed steps for the two search maneuvers. Test results are presented in the subsequent results section.

#### B. Global search

In the first kind of tests, the satellites use relative position measurements as well as global attitude knowledge (“global search”). The two satellites find each other without a prior knowledge of the other satellite’s position, and point their  $-x$  face (beacon face) directly toward the other satellite. These maneuvers represent the stage (1) and (2) described above. The present global search strategy consists of the following five maneuver phases.

- (Phase 0) Starting with the initial condition such as illustrated in Figure 4, both satellites control their attitude to the ones prescribed in the inertial (global) coordinate frame as illustrated in Figure 6. The satellite is first commanded to tilt its body  $z$ -axis by 60 degrees with respect to the inertial  $Z$ -axis.

(Phase 1) Both Primary and Follower search for the partner simultaneously through a coordinated rotation. Figure 7(a) illustrates the search rotations used in this global search. The satellite rotates about the body  $z$ -axis at  $2\pi/20$  rad/s. And also it rotates about the body  $y$ -axis at  $2\pi/120$  rad/s by 120 deg, and then rotates backward by 120 deg at the same rotation rate. As illustrated in

- Figure 6, two satellites rotate in the opposite direction so that the two satellites find each other approximately at the same time.
- (Phase 2) One of the satellites notifies the other satellite of reception of the U/S signal using a direct satellite-to-satellite communication.
- (Phase 3) The satellite who received the U/S signal from the partner starts the state estimation using the single U/S signal emitted from the partner. (This estimator is called “the relative estimator” hereafter.) Then points its beacon-transmitter ( $-x$ ) face toward the partner. In the global search strategy, the global attitude information is also used so that the body  $z$ -axis makes the minimum angle from the inertial  $Z$  axis while the satellite points the beacon face toward the partner. In a real distributed-satellite system, a star tracker will provide such global attitude estimation.
- (Phase 4) Once the other satellite receives the U/S signal, it also estimates the relative states, and then points the beacon transmitter ( $-x$ ) face toward the partner. Again, the global attitude information is used so that the body  $z$ -axis in the final attitude makes the minimum angle from the inertial  $Z$  axis.

The position of the satellite is, on the other hand, actively controlled during the test with respect to the inertial coordinate frame fixed to ISS in order to avoid the drift of the satellite. Note that this global position information was not used for the search maneuvers. Throughout the tests, simple PID controllers were used both for attitude and position control.

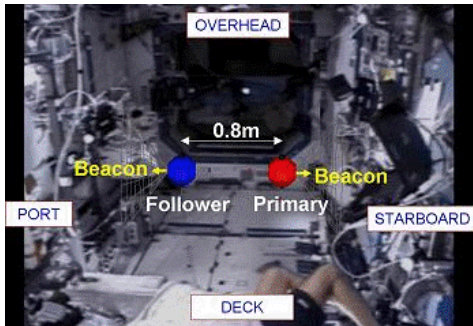


Figure 4: Initial conditions for “relative search” test

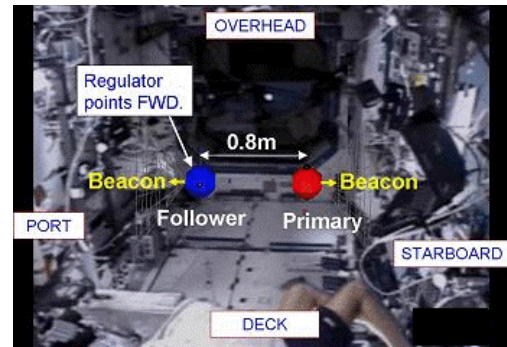


Figure 5: Initial conditions for “relative search” test

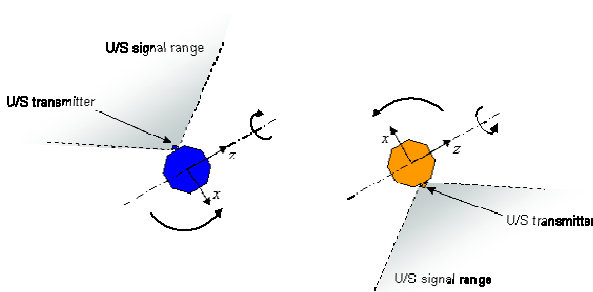


Figure 6: Coordinated search maneuver using two satellites in “global search”

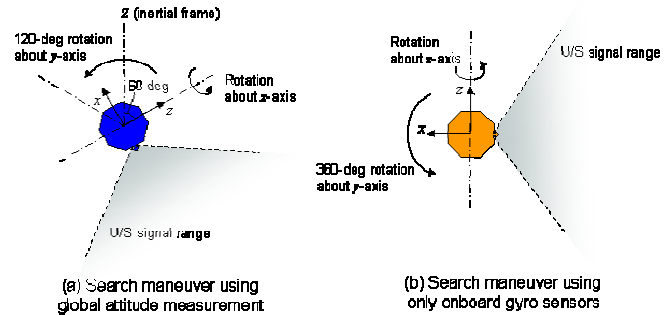


Figure 7: Two kinds of search maneuvers: (a) global search, (b) relative search

### C. Relative search

In the second kind of tests, each satellite captures the other satellite in the middle of their U/S signal range only using relative measurement (“relative search”) by the following maneuver phases.

- (Phase 1) An initial condition was chosen such as illustrated in Figure 5. The Primary satellite searches for the other satellites through a prescribed rotation. This search maneuver is illustrated Figure 7(b). The

satellite rotates at  $2\pi/20$  rad/s about the body  $z$ -axis, and also rotates at  $2\pi/120$  rad/s about the body  $y$ -axis simultaneously. The satellite only uses the onboard gyro sensor to perform this maneuver, that is, no external beacons located inside ISS are used for attitude determination. The satellite's attitude is estimated through the integration of angular velocities measured by the onboard gyro sensors.

- (Phase 2) The Follower satellite notifies the Primary of reception of the U/S signal using a direct satellite-to-satellite communication.
- (Phase 3) The Follower satellite starts the relative state estimation using the single U/S signal emitted from the Primary. Then the Follower points its beacon-transmitter ( $-x$ ) face toward the Primary according to the relative estimation.
- (Phase 4) Once the Primary receives the U/S signal emitted from the Follower, the Primary also estimates its states relative to the Follower, and then points the beacon-transmitter ( $-x$ ) face toward the Follower.

As in the global search, the positions of the satellites are actively controlled using the global estimator to avoid an undesired drift of the satellites.

## D. Results

### Global search

Figure 8(a) displays the time history of the angle between the relative position vector that points from the Primary to the Follower and the body  $-x$  axis (beacon face) of the Primary. Figure 9 shows the two vectors and the angle between them. This angle represents a pointing error. Similarly, Figure 8(b) shows the pointing error for the Follower satellite. These angles are calculated using global state estimates sent from the satellites during the test. The crew initially positioned the two satellites facing away from each other, as displayed in Figure 3, with the pointing errors of 160 deg for the Primary and of 151 deg for the Follower. (Figure 8 shows the angles only after  $t = 15$  s since the first 15 s is allocated for the convergence of the global estimator.) The errors decreased almost monotonically through the present global search strategy. After  $t = 60$  s, the pointing errors were less than 10 deg for both satellites.

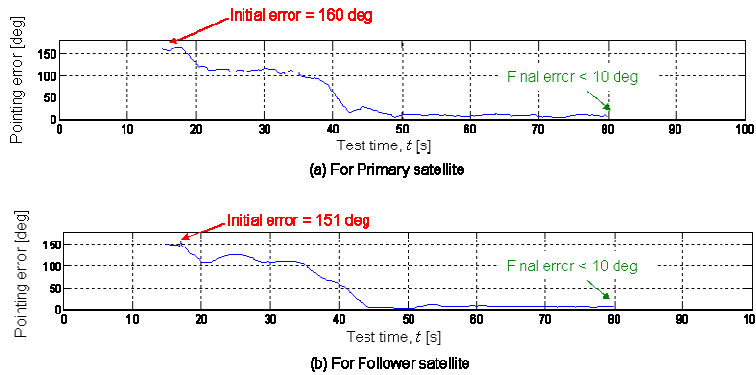


Figure 8: Pointing angle error in each satellite during “global search” test

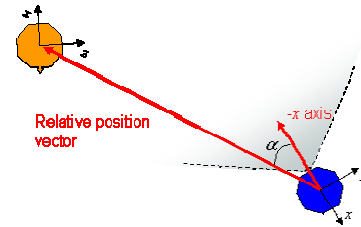


Figure 9: Pointing-error angle  $\alpha$  between the pointing vector and the U/S transmitter direction ( $-x$ )

Figure 10 and Figure 11 display the telemetry data sent from the two satellites during the global search test. Figure 10(a) shows the Primary satellite's attitude and rotation rate with respect to the inertial coordinate frame, estimated by the global estimator. Figure 10(b) shows the Primary satellite's position and velocity in the body coordinate frame, estimated by the single beacon relative estimator. Figure 11(a) and (b) shows the data for the Follower satellite. The Euler quaternion parameters ( $q_1, q_2, q_3, q_4$ ) are used for the attitude representation where  $q_4$  is the real part of the quaternion. The pink vertical lines, shown as “Man” in the legend, display the maneuver sequence transition. After the convergence of the global estimator, both satellites rotated to the prescribed attitudes illustrated in Figure 5 (Phase 0). Starting at  $t = 32$  s, both satellites carried out the coordinated search maneuver (Phase 1). At  $t = 34.7$  s, the Primary satellite received the U/S signal emitted from the Follower and sent a flag to the Follower via the satellite-to-satellite communication (Phase 2); at the same time, the Primary initiated the relative estimation (Phase 3), as can be seen in Figure 10(b). At  $t = 35.3$  s, the Follower received the U/S signal emitted from the Primary, starting the relative estimation (Phase 4) as displayed in Figure 11(b). Using the relative estimation as well as the global attitude information, the satellites pointed the beacon ( $-x$ ) face toward each other, achieving the pointing error within 10 deg as shown in Figure 9. Figure 12 displays the angle between the body  $z$ -axes of the two satellites during the test. This angle is calculated using the data given by the global estimators. The final attitude is

controlled in this test so that the body  $z$ -axis makes the minimum angle from the inertial  $Z$  axis while the beacon ( $-x$ ) face points toward the other satellite. As a result, the body  $z$ -axes of the two satellites will be aligned regardless of the initial conditions if the relative and global estimations were ideal. Figure 12 shows the alignment error was within 15 deg in this test. The test successfully demonstrated the present global search strategy using the hardware in the 3D ISS environment.

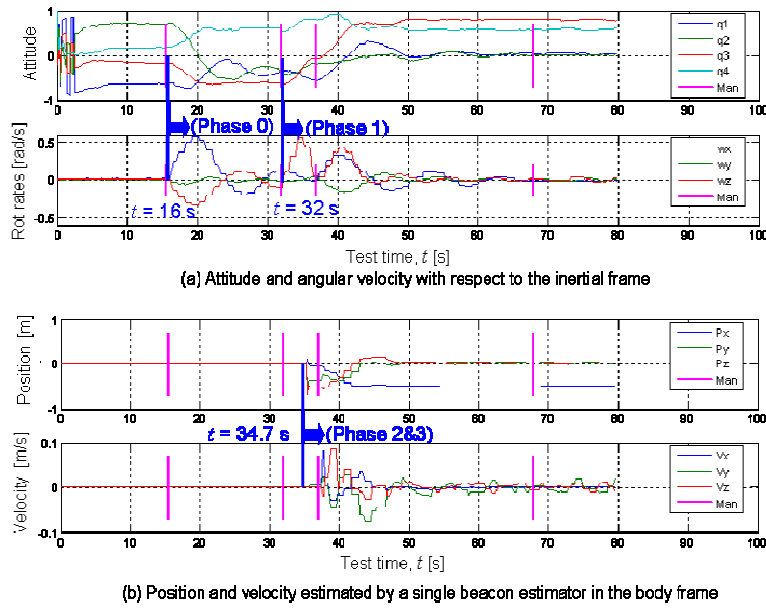


Figure 10: Telemetry data from the Primary satellite during "global search" test

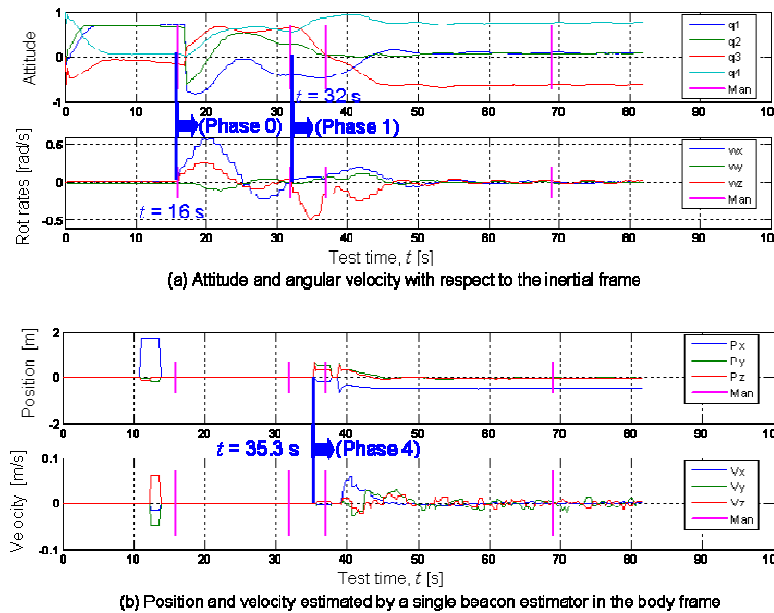


Figure 11: Telemetry data from the Follower satellite during "global search" test

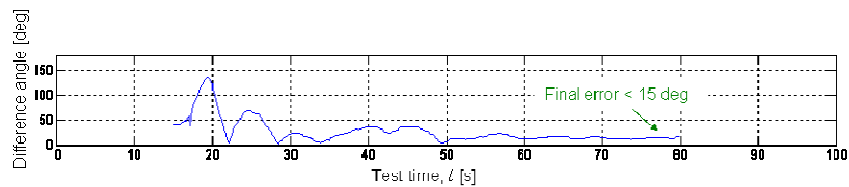


Figure 12: Angle between body  $z$ -axes of the two satellites during "global search" test

## Relative search

This test is designed to demonstrate the formation initialization by using two satellites with only onboard relative measurements (“relative search”). The two satellites successfully formed a formation also by the relative search strategy. Figure displays the initial condition for this test. Figure 13(a) and (b) shows the time history of the pointing-error angle, defined in Figure 9, for the Primary and the Follower respectively. Since the crew was asked to position the two satellites facing away from each other, the pointing errors were initially 167 deg for the Primary and 158 deg for the Follower. By the present relative search strategy, the two satellites successfully found each other and pointed to each other, making the pointing errors within 5 deg for both satellites after  $t = 60$  s.

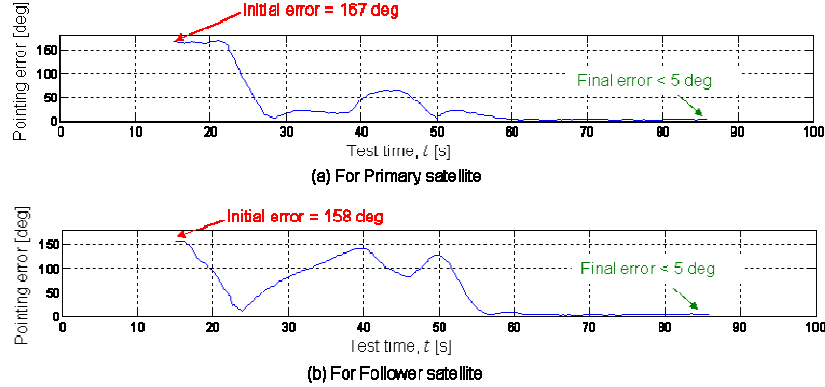


Figure 13: Pointing-error angle in each satellite during “relative search” test

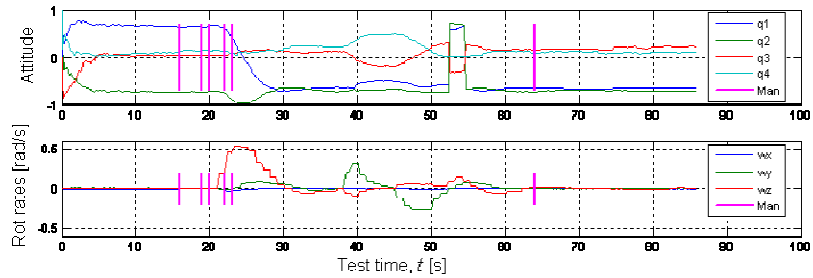
However, the close examination of the test results indicates that there was a multi-path problem of the U/S signal during this test. Figure 13 displays the Primary satellite’s data obtained during this relative search test. Figure 14(a) shows the Primary satellite’s attitude and rotation rate with respect to the inertial coordinate frame, estimated by the global estimator. Figure 14(b) shows the Primary satellite’s position and velocity in the body coordinate frame, estimated by the single beacon relative estimator. Figure 15 shows the data for the Follower satellite. As seen in Figure 15(b), the Follower carried out the relative estimation between  $t = 0$  and 4.5 s and also after  $t = 10.1$  s by receiving the U/S signal from the Primary satellite. However, the U/S transmitter (-x) face of the Primary satellite is initially pointed away from the Follower as shown in Figure 13. This suggests that the U/S signal was reflected on an ISS wall. As a result, the Follower’s relative estimator converged to a proper state only after  $t \sim 55$  s, enabling the pointing maneuver. The Follower sent a flag to the Primary via the direct satellite-to-satellite communication channel at  $t = 16$  s (Phase 2), and carried out the pointing maneuver (Phase 3). At  $t = 19.3$ , the Primary received the U/S signal emitted from the Follower and started the relative estimation (Phase 4) as seen in Figure 14(b). Although the estimator did not converge quickly due to the Follower’s unstable attitude, it converged to a proper state after  $t \sim 58$  s. Consequently, as seen in Figure 14(a) and Figure 15(a), the attitudes of both Primary and Follower were properly controlled and the rotation rates were nullified. As Figure 13 shows, the pointing errors were less than 5 deg for both satellites.

Figure 16 displays the time history of the angle between the Primary’s body  $z$ -axis and the Follower’s body  $z$ -axis. As mentioned above, the present relative search strategy does not control the rotational orientation of the satellite along the body  $x$ -axis. Hence, the body  $z$ -axes of the two satellites do not necessarily align. As Figure 16 shows, the angle was converged to approximately 20 deg in this test. This angle should vary depending upon initial conditions and disturbances during the tests. For example, the same relative search strategy was used in the test with translation (Section VI.D) and this angle was approximately 85 deg in the end of the test. Although there was a multi-path problem of the U/S signal, the test successfully demonstrated the adequacy of the present relative search strategy.

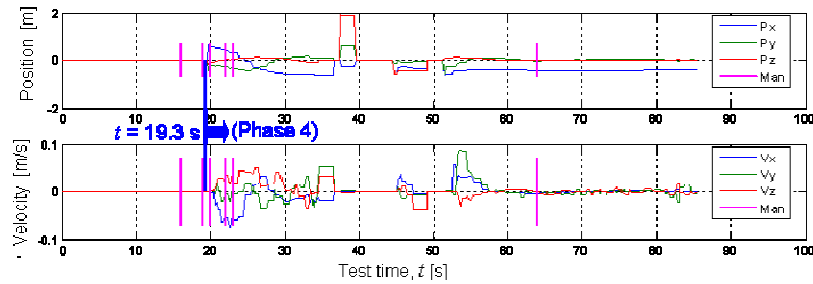
### A. Global search with translation

This test was designed to demonstrate that the present global search strategy is effective even when two satellites have a moderate relative translational velocity. Figure 17 shows the initial condition for the test. With this initial condition, the global search strategy in Section VI.A was repeated; but this time, the Follower satellite was commanded to translate in the inertial +Z direction (toward the DECK) with a 0.02 m/s velocity. Figure 18 displays the time history of the pointing errors of the two satellites during the test. As seen in the figure, the two satellites

initially faced away from each other and, through the present search strategy, they successfully pointed each other within a 25 deg error for the Primary and within a 15 deg error for the Follower.

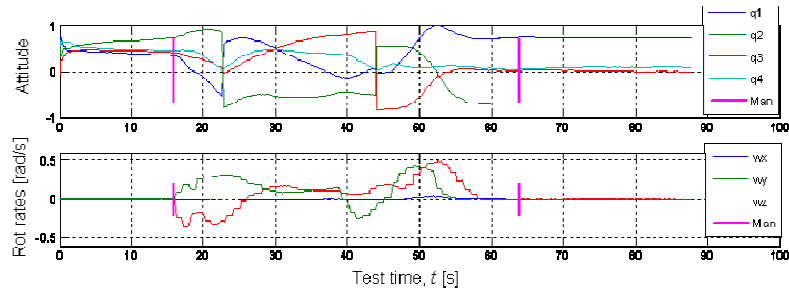


(a) Attitude and angular velocity with respect to the inertial frame

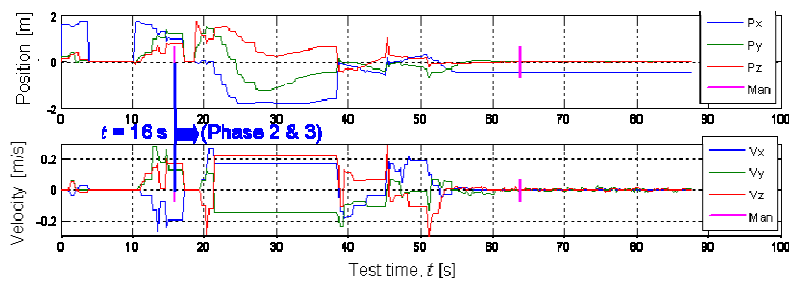


(b) Position and velocity estimated by a single beacon estimator in the body frame

Figure 14: Telemetry data from the Primary satellite during “relative search” test



(a) Attitude and angular velocity with respect to the inertial frame



(b) Position and velocity estimated by a single beacon estimator in the body frame

Figure 15: Telemetry data from the Follower satellite during “relative search” test

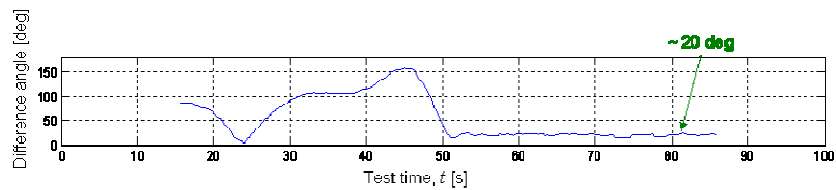


Figure 16: Angle between body  $z$ -axes of the two satellites during “relative search” test

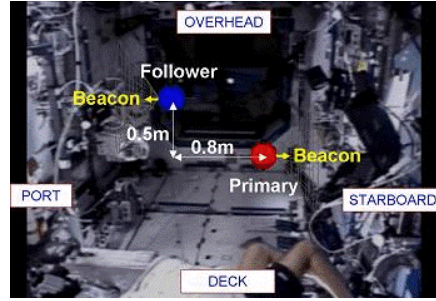


Figure 17: Initial condition for “global search with translation” test and “relative search with translation” test

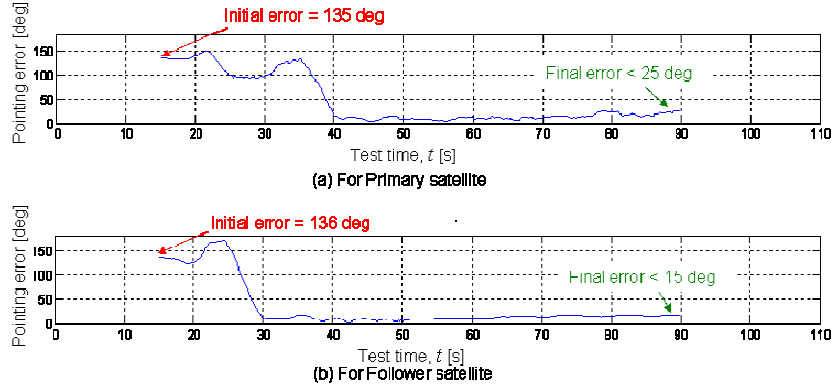


Figure 18: Pointing angle error in each satellite during “global search with translation” test

Figure 19 and Figure 20 illustrate the global estimation data sent from the Primary and the Follower, respectively. As seen in the top plot of Figure 20, the Follower started the translation in the inertial +Z direction at  $t = 16$  s and was commanded to stop the translation at  $t = 75$  s in order not to hit the wall. In this test, the Follower began receiving the U/S signal from the Primary at  $t = 5.1$  s when the Primary still pointed the beacon face away from the Follower. This indicates that the U/S signal was reflected on the ISS wall. As a result, the relative estimator did not converge quickly, but converged to a proper state only after  $t \sim 45$  s. After  $t \sim 45$  s, both satellites successfully pointed each other even when there was a translational velocity up to  $t = 75$  s. Figure 21 displays the angle between the body z-axes of the two satellites. As explained in Section IV.B, the present global-search strategy uses the global attitude knowledge for attitude control. The plot shows that the two axes aligned within 15 deg difference.

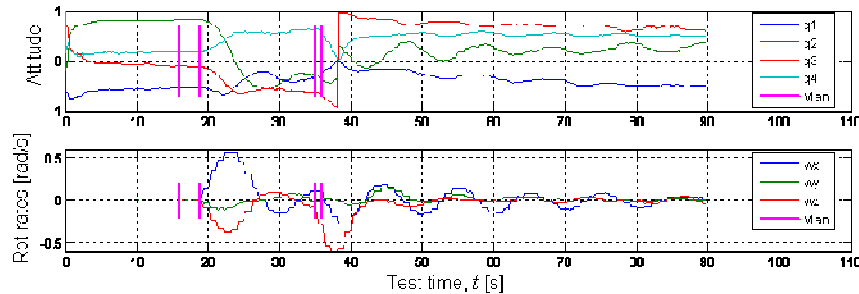


Figure 19: Telemetry data from the Primary satellite during “global search with translation” test

## B. Relative search with translation

This test was designed to demonstrate that the present relative-search strategy is effective even when the two satellites have a moderate relative translational velocity. Figure 17 shows the initial condition for the test. The relative-search strategy in Section VI.B was repeated; but this time, the Follower satellite was commanded to translate in the inertial +Z direction (toward the DECK) with a 0.02 m/s velocity. Figure 22 displays the time history of the pointing errors of the two satellites during the test. As seen in the figure, the two satellites initially faced away from each other, and then, through the present search strategy, they successfully pointed each other within a 15 deg error for the Primary and within a 10 deg error for the Follower.

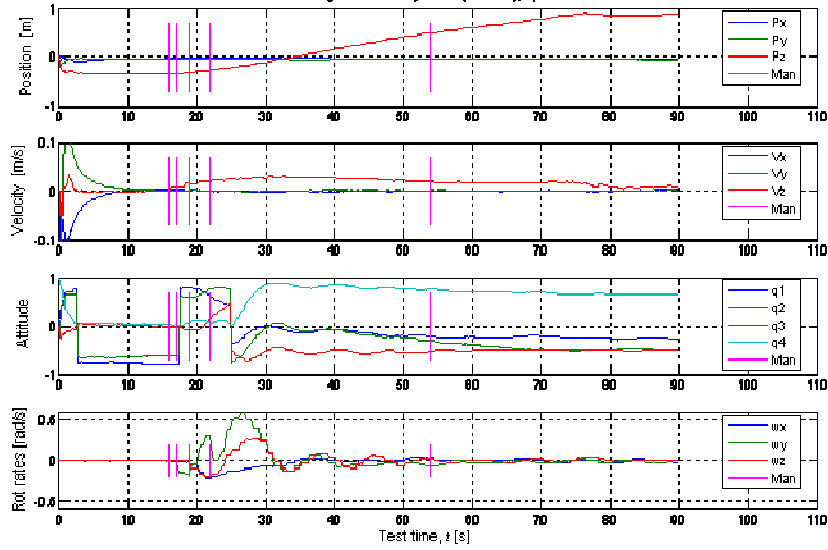


Figure 20: Telemetry data from the Follower satellite during “global search with translation” test

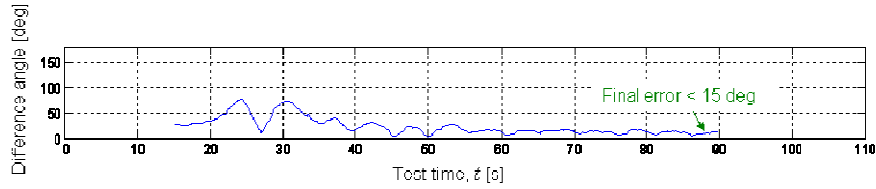


Figure 21: Angle between body  $z$ -axes of the two satellites during “global search with translation” test

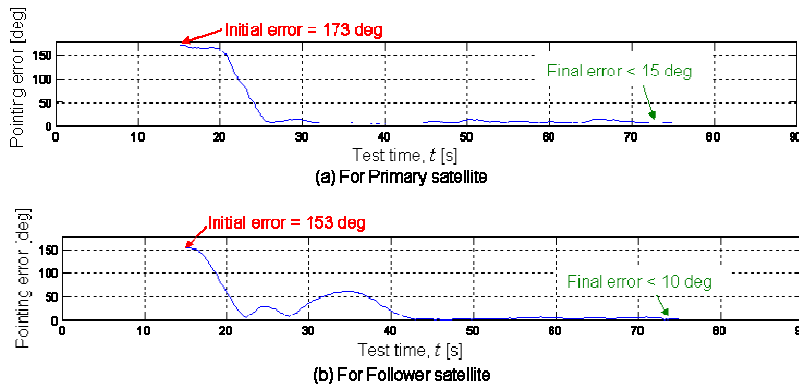


Figure 22: Pointing angle error in each satellite during “relative search with translation” test

Figure 23 and Figure 24 illustrate the global estimation data sent from the Primary and the Follower, respectively. As seen in the top plot of Figure 23, the Follower started the translation in the inertial  $+Z$  direction at  $t = 16$  s and was commanded to stop the translation at  $t = 75$  s. In this test, the Follower began receiving the U/S signal from the Primary at  $t = 3.1$  s due to the multi-path problem. The relative estimator on the Follower converged to a proper state only after  $t \sim 45$  s. After  $t \sim 45$  s, both satellites successfully pointed each other even when there was a translational velocity up to  $t = 75$  s. Figure 25 displays the angle between the body  $z$ -axes of the two satellites. As explained in Section IV.C, the present relative-search strategy does not control the rotational orientation about the body  $x$ -axis while pointing the  $-x$ -face toward the other satellite. Therefore, the angle between the body  $z$ -axes of the two satellites varies depending upon initial conditions and disturbances. In this test, the angle was approximately 85 deg.

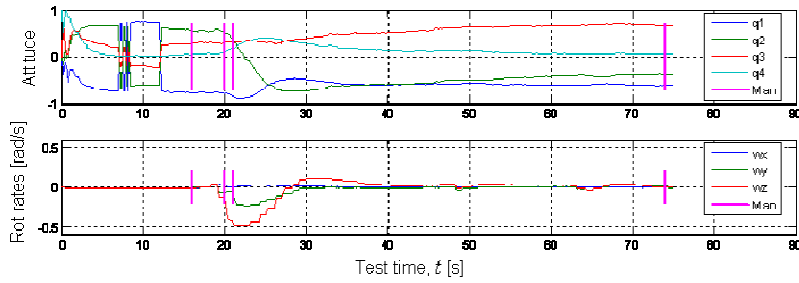


Figure 23: Telemetry data from the Primary satellite during “relative search with translation” test

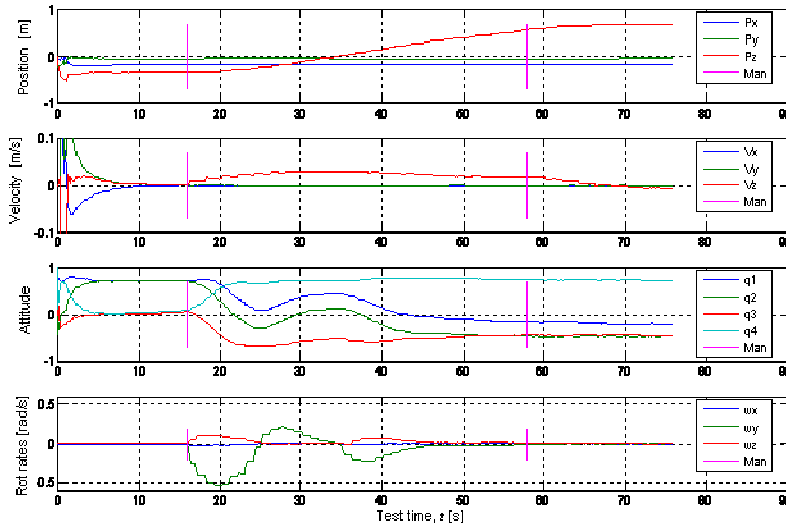


Figure 24: Telemetry data from the Follower satellite during “relative search with translation” test

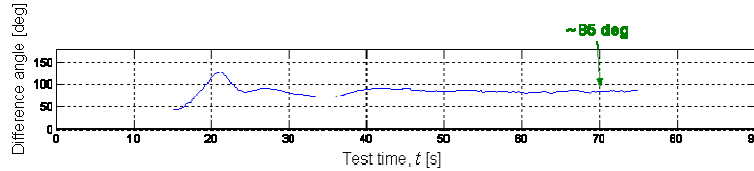


Figure 25: Angle between body z-axes of the two satellites during “relative search with translation” test

#### IV. Formation Control

A formation flight mission is evaluated by a tradeoff between two metrics: its scientific output and its cost. Both these metrics depend on the same quantities: fuel usage and required time. As fuel usage increases, the potential mission duration is shortened, decreasing operational costs but also capping scientific output. If on-orbit refueling is possible, then scientific results may not be compromised but the overall mission cost will increase. Required flight time increases the total operations cost of the mission as well as decreasing the density of scientific operations, for maneuvers which only enable results such as the repointing of an interferometric array. It must be noted that it is not optimal to minimize fuel usage, as this often results in one satellite performing most of the required motion while others coast to targets with little control. But if a single satellite runs out of fuel, the mission itself can be compromised even though all other satellites are still fully functional. Since formation flight missions generally require the spacecraft to achieve a certain configuration relative to each other, with no constraint on their absolute position in an externally defined reference frame, fuel can be balanced in the formation by changing the amount of maneuvering done by each satellite while maintaining their relative configurations.

##### A. Trajectory optimization

There are several equivalent ways to achieve fuel balancing between satellites. Reference [7] provides an elementary approach to the problem and determines optimal trajectories that attempt to create equal fuel usage

among different spacecraft tracking a trajectory. However if the satellites don't start with the same amount of propellant in their tanks, the maneuvers won't balance fuel among them.

When propellant use is proportional to control command, as is most often the case, a simple way to drive the propellant level in all spacecraft to the same value is to extend the state vector of the system: if  $x_i$  denotes the state (position and velocity) of the  $i$ -th component of the formation, obeying  $\dot{x}_i = Ax_i + Bu_i$  with  $u_i$  the control command; and  $p_i$  the level of propellant in the  $i$ -th satellite then the new state vector  $y = [x_1^T \cdots x_i^T \cdots x_n^T \ p_1 \ \cdots \ p_i \ \cdots \ p_n]^T$  obeys the dynamics:

$$\dot{y} = \begin{bmatrix} A & & 0 \\ & \ddots & \\ 0 & & A \\ 0 & \cdots & 0 \\ & \ddots & \\ 0 & \cdots & 0 \end{bmatrix} y + \begin{bmatrix} B & & 0 \\ & \ddots & \\ -F & & B \\ & \ddots & \\ 0 & & -F \end{bmatrix} [u_1 \ \cdots \ u_i \ \cdots \ u_n] \quad (1)$$

with  $\Delta p_i = Fu_i$  the amount of fuel consumed for a command of  $u_i$ . This allows to use standard optimal control methods to determine optimal trajectories that optimize:

$$J = \alpha_f + \int_{t_0}^{t_f} \left( y^T Q y + \sum_{j=1}^n u_j^T R u_j \right) dt \quad (2)$$

with  $\alpha$ ,  $R$  and  $Q = \beta$   $\begin{bmatrix} & & & 0 \\ & n & -1 & \cdots & -1 \\ -1 & & n & \ddots & -1 \\ \vdots & & \ddots & \ddots & \vdots \\ -1 & -1 & \cdots & & n \end{bmatrix}$  the cost weight parameters on time, fuel consumption and fuel

balancing respectively; subject to constraints on initial positions, relative position over time (a function of  $(x_i - x_j)$ ) and control limitations ( $|u_i| \leq u_{\max}$ ). Figure 27 shows the resulting trajectory for three spacecraft required to maintain an equilateral triangle while rotating in a circle around the center of the triangle, with  $p_1 = 1/2$ ,  $p_2 = 1$  and  $p_3 = 1$  and  $\alpha = 0$ ,  $R = I$  and  $\beta = 1$  as well as constrained final time.

## B. Trajectory Coordination

Reference [8] describes an elegant non-linear tracking controller for curved trajectories, which significantly outperforms classical controllers on spirals and circles, the standard trajectories for planar distributed interferometers. For each satellite, the guidance logic determines the points on the trajectory at a pre-selected distance  $L$  from the satellite. There are nominally two such points. The controller then selects the forward point on the trajectory and applies a lateral acceleration command corresponding to the centripetal acceleration the satellite would be subjected to if it were following a circular trajectory passing through its current location and the selected point, with its current velocity tangential to the trajectory. This controller is proven to be Lyapunov-stable for circular trajectories in reference [9].

As this algorithm is particularly simple and computationally very light, it has great appeal for formation flight applications. When the satellite is on the desired trajectory, the commanded acceleration is exactly the centripetal acceleration required to describe a circle of the desired radius. As a result, if two satellites are tracking the same trajectory, they will be describing circles with angular rates corresponding exactly to the speed they had as they reached a point on the trajectory for the first time. But as synchronization between the different components of an

interferometer is crucial for optimal image resolution, the guidance logic has to be extended to take the time-sensitivity of the satellites' motion into account.

Synchronizing the formation's trajectory can be done by either communicating states between certain satellites in the formation, or by including a time-component in the described trajectory itself. To benefit from the computational simplicity of this algorithm we've taken the latter approach. Our algorithm selects the forward point on the desired trajectory at a distance  $L$  from the current position of the craft. It then determines the difference in time  $\Delta t$  between the current time and the time at which the craft should be at the selected point on the trajectory. In addition to a lateral acceleration command ( $a_{\perp}$ ), we apply an additional acceleration ( $\Delta V_{\parallel}$ ) to increase the craft's angular rate along an imaginary circle that would encompass the craft's current position, the selected target position and in such a way that it would pass from one to the other over a time  $\Delta t$  :

$$R = \frac{L}{2 \sin \eta}$$

So

$$\Delta V_{\parallel} = \frac{\eta L}{\Delta t \sin \eta} - V$$

And

$$a_{\perp} = \frac{(V + \Delta V_{\parallel})^2}{R} = \frac{2\eta^2 L}{\Delta t^2 \sin \eta}$$

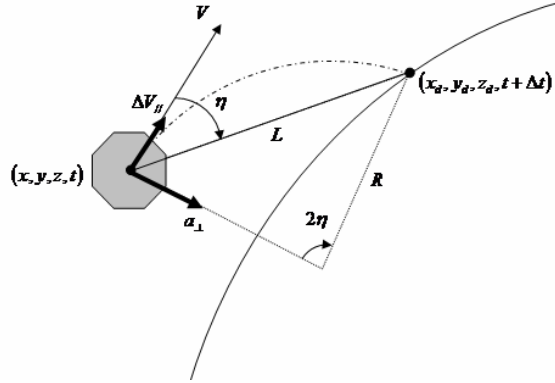


Figure 26: Diagram of the parameters for the synchronizing controller

$L$  acts as a gain for the controller and has to be determined to avoid singularities due to lags in the system causing  $\Delta t$  to vanish.

If the trajectory is simple enough, the satellite can be synchronized in an even more successful manner: a desired speed profile can be determined for the time-critical trajectory of each satellite. It is then possible to construct a 4-dimensional curve by mapping the desired trajectory  $T_d \equiv (x_d, y_d, z_d, t_d)$  on to  $\tilde{T}_d \equiv (x_d, y_d, z_d, \|V_d(t_d)\|t_d)$ .

This suggests a similar algorithm in which we find the two points on  $\tilde{T}_d$  at a distance  $L$  from our current position  $(x, y, z, \|V\|t)$ . Picking the forward one, we apply the same commands as before using  $\Delta t = t_d - t$ . Figure 28 displays the relative position of two satellites following a circle using the above control logics.

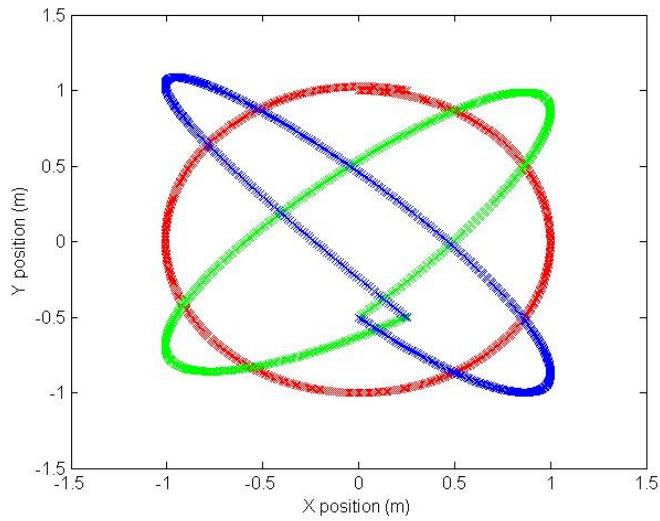


Figure 27: Fuel balanced trajectory for three satellites performing a circular maneuver with different initial propellant levels

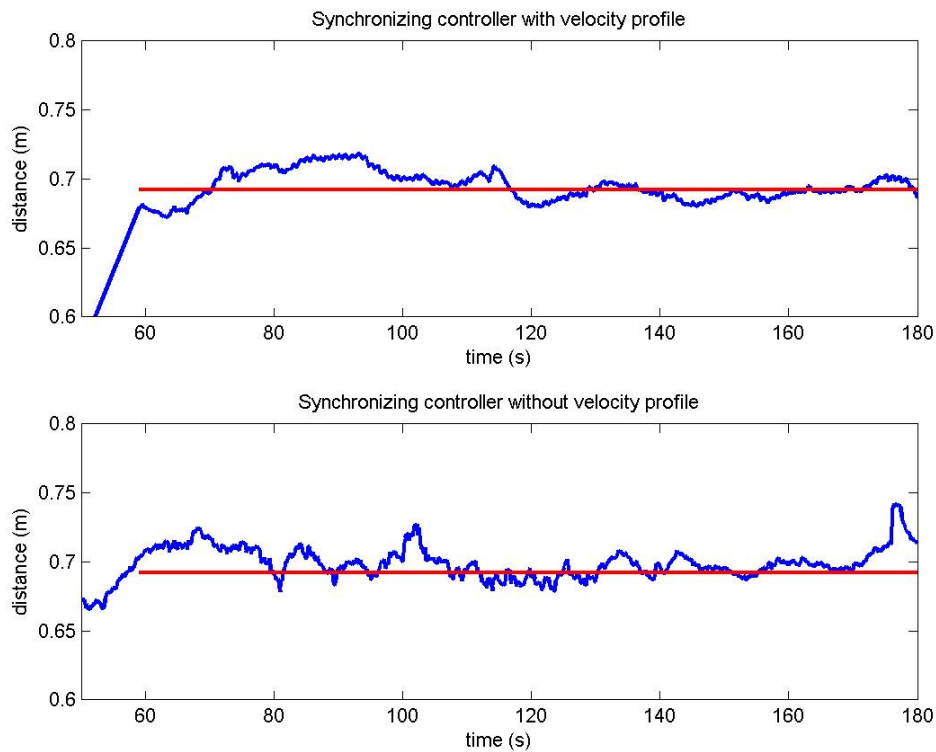


Figure 28: Relative distance between two satellites following a circular trajectory using the synchronized controllers with (top) and without (bottom) predefined velocity profiles.

## V. Conclusions

In this paper we've presented an approach to three fundamental aspects of formation flight: achieving the initial formation without knowledge of the position of other members of the formation, generating trajectories that optimize the mission's purpose by balancing fuel among the different and tracking the generated trajectories in a synchronized fashion. Experimental results from tests performed in the space station were analyzed for the formation acquisition problem.

Future work includes developing the formation acquisition problem for more than two satellites, determining stability margins for the synchronizing controllers and integrating all three problems to demonstrate full mission profile performance.

### References

1. E. M.-C. Kong, *Spacecraft Formation Flight Exploiting Potential Fields*, PhD Thesis, Massachusetts Institute of Technology, Feb. 2002.
2. Terrestrial Planet Finder Interferometer artist concept.  
<http://planetquest.jpl.nasa.gov/gallery/tpfBrowseImages.html>
3. A. Saenz-Otero and D. Miller. "SPHERES: a platform for formation-flight research," UV/Optical/IR Space Telescopes: Innovative Technologies and Concepts II conference, San Diego, CA, August 2005.
4. F. Hadaegh, D. Scharf, and S. Ploen, "Initialization of Distributed Spacecraft for Precision Formation Flying," IEEE Conf. Control Applications, Istanbul, Turkey, June 2003.
5. D. Scharf, S. Ploen, F. Hadaegh, J. A. Keim, and L. H. Phan, "Guaranteed Initialization of Distributed Spacecraft Formations," AIAA-2003-5590, AIAA Guidance, Navigation, and Control Conference and Exhibit, Austin, TX, Aug. 11-14, 2003.
6. D. Scharf, S. Ploen, F. Hadaegh and G. Sohl, "Guaranteed Spatial Initialization of Distributed Spacecraft Formations," AIAA-2004-4893, AIAA Guidance, Navigation, and Control Conference and Exhibit, Providence, RI, Aug. 16-19, 2004.
7. A. Rahmani, M. Mesbahi and F. Y. Hadaegh, "Optimal Balanced-Energy Formation Flying Maneuvers", *J. Guidance, Control and Dynamics*, 29 (6), pp. 1395-1403, 2006.
8. S. Park, J. Deyst and J. P. How, "A New Nonlinear Guidance Logic for Trajectory Tracking", AIAA Guidance, Navigation and Control Conference and Exhibit, Providence, RI, Aug. 16-19, 2004
9. J. Deyst, J. P. How and S. Park, "Lyapunov Stability of a Nonlinear Guidance Law for UAVs", AIAA Guidance, Navigation and Control Conference and Exhibit, San Francisco, CA, Aug. 15-18, 2005